Resonant Diffusion of a Gravitactic Circle Swimmer

Oleksandr Chepizhko and Thomas Franosch
Institut für Theoretische Physik, Universität Innsbruck, Technikerstraße 21A, A-6020 Innsbruck, Austria

(Received 23 March 2022; revised 16 August 2022; accepted 7 October 2022; published 23 November 2022)

We investigate the dynamics of a single chiral active particle subject to an external torque due to the presence of a gravitational field. Our computer simulations reveal an arbitrarily strong increase of the long-time diffusivity of the gravitactic agent when the external torque approaches the intrinsic angular drift. We provide analytic expressions for the mean-square displacement in terms of eigenfunctions and eigenvalues of the noisy-driven-pendulum problem. The pronounced maximum in the diffusivity is then rationalized by the vanishing of the lowest eigenvalues of the Fokker-Planck equation for the angular motion as the rotational diffusion decreases and the underlying classical bifurcation is approached. A simple harmonic-oscillator picture for the barrier-dominated motion provides a quantitative description for the onset of the resonance while its range of validity is determined by the crossover to a critical-fluctuation-dominated regime.

DOI: 10.1103/PhysRevLett.129.228003

Active particles capable of self-propulsion by converting energy into directed motion have come into research focus and are important from both a fundamental and an applied point of view [1–5]. Examples for active agents include various motile organisms, in particular bacteria [6–8] or algae [9], as well as artificial realizations such as Janus rods [10], spheres [11], or Quincke rollers [12]. Recently, significant advances in our understanding of transport properties of active motion in homogeneous environments [4,13–18] and in media crowded with obstacles [19–25] have been achieved.

External fields, torques, and gradients induce various forms of *taxis* such as chemotaxis [26,27], magnetotaxis [28,29], gravitaxis [30], rheotaxis [31], or viscotaxis [32] due to a combination of the persistence of motion and different noise sources [1,4]. Already the case of a homogeneous force field such as gravity gives rise to counterintuitive dynamics by coupling to the orientational motion. For systems of L-shaped chiral microswimmers [33] and Janus rods [34], mass-anisotropic colloids [35,36], and microorganisms [30] gravitaxis has been demonstrated experimentally. In particular, these experiments have discovered that chiral active particles subject to a gravitational field can move upwards, which was also supported by simulation studies in bottom-heavy microswimmers [37] and chiral swimmers [38]. Experimental studies of sedimenting active particles revealed an enhancement of diffusivity by activity [39], while an analytical solution for the density profile has been obtained only recently [40]. The sedimentation profile of active particles was also studied in detail in computer simulations and experiments with Janus particles [41] as well as for run-and-tumble particles [42]. Yet, the temporal dynamics and transport properties such as the mean-square displacement and the corresponding diffusivity have not been elucidated in detail.

In this Letter, we demonstrate by computer simulation that gravitaxis of circle swimmers displays resonant diffusivities for small orientational diffusion as the gravitational torque approaches the intrinsic angular drift velocity. We then elaborate a complete analytical solution of gravitactic motion for the model developed by ten Hagen *et al.* [33]. A formal expression for the intermediate scattering function, encoding the spatiotemporal motion, is derived. Using a time-dependent perturbative approach we extract the mean drift and the mean-square displacement. Our analytic results reveal that the resonance is encoded in the vanishing of the eigenvalues of the associated Fokker-Planck operator. We rationalize the onset of the resonance within a harmonic approximation and determine the growth of the maximum of the resonance by crossover scaling.

Model.—We rely on the model derived in Ref. [33] for an active chiral particle subject to an external (gravitational) field. The particle moves at constant speed v along a direction $\mathbf{u}(t) \coloneqq (\cos\vartheta(t), \sin\vartheta(t))$ parametrized by a time-dependent angle $\vartheta(t)$ measured from the horizontal

$$\dot{\mathbf{r}}(t) = v\mathbf{u}(t) = v(\cos\vartheta(t), \sin\vartheta(t)). \tag{1}$$

The evolution of $\vartheta(t)$ is governed by two contributions. The external field results in an angle-dependent torque aligning the orientation in a certain direction. The coating of the active particle is such that with this orientation the self-propulsion is horizontal. Additionally, the anisotropy of the particle induces an internal angular drift $\omega > 0$ resulting in the equation of motion

$$\dot{\vartheta}(t) = \omega - \gamma \sin \vartheta(t) + \zeta(t). \tag{2}$$

Here, the torque γ is proportional to the external force and $\zeta(t)$ is a centered Gaussian white noise $\langle \zeta(t)\zeta(t')\rangle = 2D_{\mathrm{rot}}\delta(t-t')$, where D_{rot} is the bare orientational diffusion constant. The equations of motion are rewritten with proper substitutions from Ref. [33], where for simplicity we discard noise terms and additional drift terms due to (anisotropic) translational diffusion in Eq. (1). The neglected terms can be incorporated with little effort but do not change the overall picture of the resonance phenomenon (see Supplemental Material [43]). Without the external field the model reduces to the free circle swimmer [13,17,46,47], while for $\gamma > 0$ the angular motion corresponds to Brownian motion in a tilted washboard potential [48,49]. Ignoring the noise in Eq. (2) yields the classical dynamics of an overdamped driven pendulum displaying a saddle-node bifurcation at the critical value $\gamma_c = \omega$ [50]. The mapping of the gravitaxis problem to the noisy driven pendulum constitutes our first result.

Simulation.—The model is encoded in 4 parameters characterizing gravitaxis. We employ $1/\omega$ as fundamental unit of time, while the radius of the circular motion v/ω sets the unit of length. Then γ/ω is the dimensionless torque and D_{rot}/ω quantifies the relative importance of fluctuations. Stochastic simulations are performed and the displacement $\Delta\mathbf{r}(t) \coloneqq \mathbf{r}(t) - \mathbf{r}(0)$ is monitored in the stationary state. In particular, we extract the mean displacement $\langle \Delta\mathbf{r}(t)\rangle$ and the variance $\mathsf{Var}[\Delta\mathbf{r}(t)] \coloneqq \langle[\Delta\mathbf{r}(t) - \langle\Delta\mathbf{r}(t)\rangle]^2\rangle$.

In the stationary state the mean displacement grows linearly in time with the average velocity $v(\langle\cos\vartheta(t)\rangle, \langle\sin\vartheta(t)\rangle)$. Since the stationary distribution of the angle $p^{\mathrm{st}}(\vartheta)$ is elementary [51], the mean drift can be readily obtained by quadrature. Here, we recall that without noise, $D_{\mathrm{rot}} = 0$, the orientational angle is locked at $0 < \vartheta_* \leq \pi/2$ with $\sin\vartheta_* = \omega/\gamma$ provided the torque fulfills $\gamma \geq \omega$. If the torque is weaker than the internal drift, $\gamma < \omega$, the angular motion is periodic [50]. Directly at the classical bifurcation, the particle moves upwards against the field [52]. Upon reintroducing the noise the average horizontal motion is suppressed above the bifurcation, while below the fluctuations enable a net drift (see also Fig. S.3 in Supplemental Material [43]). The drift against the field direction is always suppressed by noise.

The variance $\mathsf{Var}[\Delta\mathbf{r}(t)]$ increases as t^2 for small times, see Fig. 1, where the prefactor decreases drastically as the torque is increased. Below the classical bifurcation characteristic oscillations emerge, similar to the free circle swimmer [17,53], while for $\gamma > \omega$ the variance increases monotonically. The long-time behavior is diffusive in the presence of noise, $D_{\mathrm{rot}} > 0$, and the diffusion coefficient is enhanced close to the classical bifurcation. The extracted long-time diffusion coefficients $D \coloneqq \lim_{t\to\infty}(1/4)\mathrm{d}\mathsf{Var}[\Delta\mathbf{r}(t)]/\mathrm{d}t$ are displayed in terms of the known diffusivity without external torque [13,17] $D_0 \coloneqq v_0^2 D_{\mathrm{rot}}/[2(D_{\mathrm{rot}}^2 + \omega^2)]$ in Fig. 2. Close

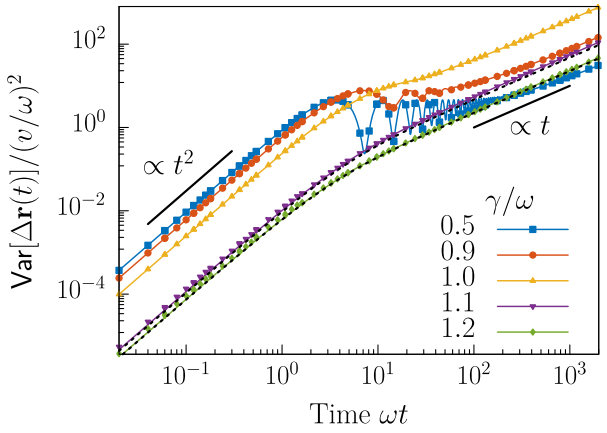

FIG. 1. Time-dependent variance $\mathsf{Var}[\Delta\mathbf{r}(t)]$ on logarithmic scales for a rotational diffusivity of $D_{\mathrm{rot}}/\omega = 0.01$ for different torques γ. Symbols correspond to simulation, the solid lines represent the analytic solution. The dotted black lines are evaluated within the harmonic-oscillator approximation, Eq. (13b), for $\gamma = 1.1\omega$ and $\gamma = 1.2\omega$. The thick black lines are power laws serving as a guide to the eye.

to the classical bifurcation a resonance emerges that becomes narrower and more pronounced as the noise is decreased.

Theory.—The goal of this part is to provide a theoretical explanation for the found resonance and to derive scaling laws in the vicinity of the classical bifurcation. The dynamical properties are encoded in the propagator $\mathbb{P}(\mathbf{r}, \vartheta, t|\vartheta_0)$, i.e., the conditional probability distribution that the particle

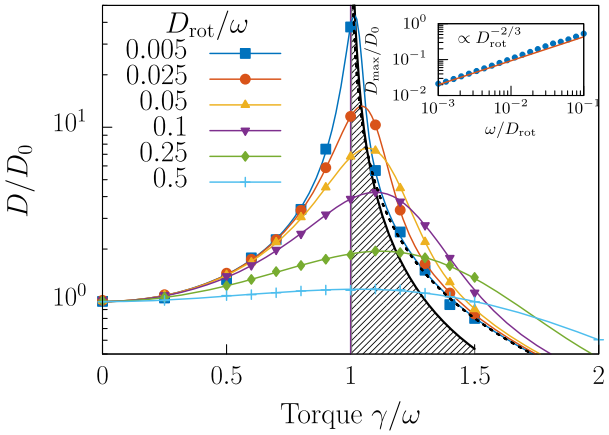

FIG. 2. Resonance of diffusivity. The diffusivity D as a function of the torque γ for different rotational diffusivities D_{rot}. The diffusivity is normalized to the diffusion coefficient of a free circle swimmer $D_0 \coloneqq v^2 D_{\mathrm{rot}}/[2(D_{\mathrm{rot}}^2 + \omega^2)]$. Symbols correspond to simulation, the full lines are analytical results. The black dotted line corresponds to the harmonic-oscillator approximation, Eq. (13b), for $D_{\mathrm{rot}} = 0.005\omega$. The right boundary of the shaded area corresponds to the parametric curve $\hat{D}_{\mathrm{rot}} \coloneqq |\gamma/\omega - 1|^{-3/2} D_{\mathrm{rot}}/\omega = \mathrm{const.}$ asymptotically intersecting the maxima of the diffusion coefficients. Inset: Increase of the maximal diffusion coefficient $D_{\max}$ for increasing inverse noise $1/D_{\mathrm{rot}}$ on logarithmic scales obtained from theory.

has displaced by $\mathbf{r}$ and its instantaneous speed exhibits an orientation ϑ at lag time t given it started with orientation ϑ_0. Angles are considered to be 2π periodic. We focus on its spatial Fourier transform $\tilde{\mathbb{P}} \coloneqq \tilde{\mathbb{P}}(\mathbf{k}, \vartheta, t|\vartheta_0) = \int d\mathbf{r} \exp(-i\mathbf{k}\cdot\mathbf{r})\mathbb{P}(\mathbf{r}, \vartheta, t|\vartheta_0)$ and derive by standard methods [51] the (Fourier transformed) Fokker-Planck equation (see also Supplemental Material [43])

$$\begin{aligned}\partial_t \tilde{\mathbb{P}} &= -\partial_\vartheta[(\omega - \gamma\sin\vartheta)\tilde{\mathbb{P}}] + D_{\mathrm{rot}}\partial_\vartheta^2\tilde{\mathbb{P}} - iv\mathbf{k}\cdot\mathbf{u}\tilde{\mathbb{P}} \\ &=: (\mathcal{L} + \delta\mathcal{L}_\mathbf{k})\tilde{\mathbb{P}}. \end{aligned} \tag{3}$$

Here the operator $\mathcal{L}$ encodes the motion of the angle, while $\delta\mathcal{L}_\mathbf{k} = -iv\mathbf{k}\cdot\mathbf{u}$ describes the coupling to the translational dynamics. The formal solution is thus $\tilde{\mathbb{P}}(\mathbf{k}, \vartheta, t|\vartheta_0) = \exp[(\mathcal{L} + \delta\mathcal{L}_\mathbf{k})t]\delta(\vartheta - \vartheta_0)$.

From this quantity the intermediate scattering function (ISF) $F(\mathbf{k}, t) = \langle\exp(-i\mathbf{k}\cdot\Delta\mathbf{r}(t))\rangle$ is obtained in the stationary state by averaging over the initial angle and integrating over the final one

$$\begin{aligned}F(\mathbf{k}, t) &= \int_0^{2\pi} \mathrm{d}\vartheta \int_0^{2\pi} \mathrm{d}\vartheta_0\, \tilde{\mathbb{P}}(\mathbf{k}, \vartheta, t|\vartheta_0) p^{\mathrm{st}}(\vartheta_0) \\ &= \int_0^{2\pi} \mathrm{d}\vartheta\, \exp[(\mathcal{L} + \delta\mathcal{L}_\mathbf{k})t] p^{\mathrm{st}}(\vartheta). \end{aligned} \tag{4}$$

Moments of the displacement can be extracted by a series expansion in the wave vector $\mathbf{k}$

$$F(\mathbf{k}, t) = 1 - i\mathbf{k}\cdot\langle\Delta\mathbf{r}(t)\rangle - \frac{1}{2}\langle[\mathbf{k}\cdot\Delta\mathbf{r}(t)]^2\rangle + \ldots. \tag{5}$$

Here we follow the strategy of Ref. [17] (see also Ref. [54]), solve the eigenvalue problem of the reference system $\mathcal{L}$, and apply time-dependent perturbation theory for $\delta\mathcal{L}_\mathbf{k}$. We denote by $\{|n\rangle : n \in \mathbb{Z}\}$ the standard orthonormal basis in the Hilbert space $L^2[0, 2\pi]$ with real-space representation $\langle\vartheta|n\rangle \coloneqq \exp(in\vartheta)/\sqrt{2\pi}$. In this basis $\mathcal{L}$ is represented in terms of its matrix elements [51]

$$\begin{aligned}\mathcal{L}_{mn} = \langle m|\mathcal{L}n\rangle &\coloneqq \int_0^{2\pi} \frac{\mathrm{d}\vartheta}{2\pi} e^{-im\vartheta}\mathcal{L}e^{in\vartheta} \\ &= (-D_{\mathrm{rot}}m^2 - im\omega)\delta_{mn} + \frac{\gamma}{2}m(\delta_{m,n+1} - \delta_{m,n-1}). \end{aligned} \tag{6}$$

In particular, the matrix representation is non-Hermitian and tridiagonal due to the torque. Right and left eigenstates $\mathcal{L}|r_\lambda\rangle = -\lambda|r_\lambda\rangle$, $\mathcal{L}^\dagger|l_\lambda\rangle = -\lambda^*|l_\lambda\rangle$ are readily obtained by numerically diagonalizing the matrix, Eq. (6), yielding the expansion coefficients $\langle n|r_\lambda\rangle$, $\langle l_\lambda|n\rangle$ as right and left eigenvector of the matrix $\mathcal{L}_{mn}$. The corresponding real-space representation is obtained by expansion $r_\lambda(\vartheta) = \sum_{n\in\mathbb{Z}}\langle\vartheta|n\rangle\langle n|r_\lambda\rangle$. By conservation of probability $\lambda = 0$ is an eigenvalue and the real-space representations of the associated eigenstates are $r_0(\vartheta) = p^{\mathrm{st}}(\vartheta)$ and $l_0(\vartheta) = 1$. Comparing with Eq. (4) we find the compact expression for the ISF

$$F(\mathbf{k}, t) = \langle l_0|\exp[(\mathcal{L} + \delta\mathcal{L}_\mathbf{k})t]r_0\rangle. \tag{7}$$

Since $\delta\mathcal{L}_\mathbf{k} = -iv\mathbf{k}\cdot\mathbf{u}$, time-dependent perturbation theory (Born series) [55]

$$\begin{aligned}e^{(\mathcal{L}+\delta\mathcal{L}_\mathbf{k})t} = e^{\mathcal{L}t} &+ \int_0^t \mathrm{d}s\, e^{\mathcal{L}(t-s)}\delta\mathcal{L}_\mathbf{k} e^{\mathcal{L}s} \\ &+ \int_0^t \mathrm{d}s \int_0^s \mathrm{d}u\, e^{\mathcal{L}(t-s)}\delta\mathcal{L}_\mathbf{k} e^{\mathcal{L}(s-u)}\delta\mathcal{L}_\mathbf{k} e^{\mathcal{L}u} \\ &+ O(\delta\mathcal{L}_\mathbf{k})^3, \end{aligned} \tag{8}$$

directly yields the moments of the series expansion in $\mathbf{k}$ as in Eq. (5). In particular, expanding to second order in $\mathbf{k}$ and squeezing in the completeness relation $\sum_\lambda |r_\lambda\rangle\langle l_\lambda| = \mathbb{1}$, the time integrals can be formally performed (see also Supplemental Material [43]). Then we read off the mean drift velocity and the variance along the direction $\mathbf{n} \coloneqq \mathbf{k}/k$

$$\mathbf{n}\cdot\frac{\mathrm{d}}{\mathrm{d}t}\langle\Delta\mathbf{r}(t)\rangle = \frac{1}{k}\langle l_0|\delta\mathcal{L}_\mathbf{k} r_0\rangle, \tag{9a}$$

$$\mathsf{Var}[\mathbf{n}\cdot\Delta\mathbf{r}(t)] = \frac{2}{k^2}\sum_{\lambda\neq 0}\frac{1 - \lambda t - e^{-\lambda t}}{\lambda^2}\langle l_0|\delta\mathcal{L}_\mathbf{k} r_\lambda\rangle\langle l_\lambda|\delta\mathcal{L}_\mathbf{k} r_0\rangle, \tag{9b}$$

and infer the associated long-time diffusion coefficient

$$D_\mathbf{n} = \frac{-1}{k^2}\sum_{\lambda\neq 0}\frac{1}{\lambda}\langle l_0|\delta\mathcal{L}_\mathbf{k} r_\lambda\rangle\langle l_\lambda|\delta\mathcal{L}_\mathbf{k} r_0\rangle. \tag{10}$$

The analytical expressions for the total variances as well as the corresponding diffusion coefficients perfectly match the simulations, see Figs. 1 and 2. The exact expressions in terms of eigenfunctions and eigenvalues suggest that at resonance the eigenvalues become smaller and smaller as the rotational diffusion coefficient is decreased, which is confirmed by numerical diagonalization (see Supplemental Material [43]).

To gain further analytical insight, we evaluate Eqs. (9) and (10) within a harmonic approximation for the motion close to the classical fixed point ϑ_*. For small $D_{\mathrm{rot}} \ll \omega$ and well above the bifurcation the fluctuations are anticipated to be small and the corresponding linearized Langevin equation reads

$$\dot{\vartheta}(t) = -\frac{1}{\tau}[\vartheta(t) - \vartheta_*] + \zeta(t), \tag{11}$$

with vanishing relaxation rate $1/\tau = \sqrt{\gamma^2 - \omega^2} \to 0$ as $\gamma\downarrow\omega$. The associated eigenvalues of the overdamped harmonic oscillator are then simply $\lambda_n = n/\tau$, $n \in \mathbb{N}_0$ [51], and indeed

they approach zero for $\gamma \downarrow 0$ (see also Supplemental Material [43]).

To leading order we replace the perturbing operator $\delta\mathcal{L}_{\mathbf{k}}$ by the complex number $iv\mathbf{k}\cdot\mathbf{u}_*$ with the fixed orientation $\mathbf{u}_* = (\cos\vartheta_*, \sin\vartheta_*)$. In this approximation, the drift velocity is nonfluctuating and assumes its classical value. In the same approximation the variance and diffusion coefficient vanish by orthogonality of the eigenstates, consistent with a purely deterministic and nonchaotic motion. To leading nontrivial order we replace

$$\delta\mathcal{L}_{\mathbf{k}} \simeq iv\mathbf{k}\cdot\mathbf{u}_* + (\vartheta-\vartheta_*)\frac{\partial}{\partial\vartheta}\delta\mathcal{L}_{\mathbf{k}}\bigg|_{\vartheta=\vartheta_*}. \tag{12}$$

Then within the harmonic-oscillator approximation, also the off-diagonal matrix elements can be evaluated analytically, in particular, their magnitude is proportional to the angular oscillator width $\langle(\vartheta-\vartheta_*)^2\rangle = \sqrt{D_{\mathrm{rot}}\tau}$ (see Supplemental Material [43] for details). Furthermore, the angular position operator $\vartheta-\vartheta_*$ induces only nonvanishing transition matrix elements in Eqs. (9b), (10) coupling the ground state to the first excited state. Therefore the sums reduce to a single term and we find the compact expressions

$$\mathsf{Var}[\mathbf{n}\cdot\Delta\mathbf{r}(t)] \simeq 2D_{\mathbf{n}}\tau\left(\frac{t}{\tau}-1+e^{-t/\tau}\right), \tag{13a}$$

$$D_{\mathbf{n}} \simeq (v\tau)^2 D_{\mathrm{rot}}(n_x\sin\vartheta_* - n_y\cos\vartheta_*)^2. \tag{13b}$$

Within the harmonic-oscillator approximation the variance is strictly proportional to D_{rot} suggesting that for sufficiently small orientational fluctuations the curves in Figs. 1 and 2 should approach a master curve. The corresponding curves are included in Figs. 1 and 2 as black dotted lines and are in quantitative agreement for small $D_{\mathrm{rot}} \ll \omega$ and $\gamma > \omega$ not too close to the bifurcation. The emergence of the resonance is thus rationalized in terms of the softening of the harmonic relaxation rate $1/\tau \to 0$ as the bifurcation is approached.

The harmonic-oscillator picture suggests that the diffusion coefficient becomes infinite directly at the bifurcation while the simulation and the full analytic expression predict a rounding with a maximal diffusivity. The picture of the harmonic oscillator should hold provided the barrier is sufficiently high such that Kramers' escape rate [51] is much smaller than the harmonic relaxation rate. In terms of the effective potential $D_{\mathrm{rot}}U(\vartheta)/k_BT = -\omega\vartheta - \gamma\cos\vartheta$ the barrier height $\Delta U := U(\pi-\vartheta_*) - U(\vartheta_*)$ reduces to

$$\frac{\Delta U}{k_BT} = \frac{4\sqrt{2}}{3}\frac{\omega}{D_{\mathrm{rot}}}\epsilon^{3/2}[1+O(\epsilon)], \tag{14}$$

where we introduced the separation parameter $\epsilon := (\gamma-\omega)/\omega$ for the distance to the bifurcation (see Supplemental Material [43] for details). This observation suggests introducing the reduced rotational diffusion coefficient $\hat{D}_{\mathrm{rot}} := |\epsilon|^{-3/2}D_{\mathrm{rot}}/\omega$ such that for $\hat{D}_{\mathrm{rot}} \ll 1, \epsilon > 0$ the harmonic approximation holds, while for $\hat{D}_{\mathrm{rot}} \gg 1$ the barrier can be crossed readily by fluctuations and the precise height of the barrier should be irrelevant. By matching the critical fluctuations to the harmonic oscillator we predict that the maximal diffusivity should occur at $\hat{D}_{\mathrm{rot}} = O(1)$ or $D_{\mathrm{rot}} \propto |\epsilon|^{3/2}$. For small $\epsilon > 0$, the relaxation time diverges as $\tau \propto |\epsilon|^{-1/2}$ and from Eq. (13b) we infer the scaling law for the maximal diffusivity

$$D_{\max}/D_0 \propto |\epsilon|^{-1} \propto D_{\mathrm{rot}}^{-2/3}, \quad \text{for } D_{\mathrm{rot}} \to 0, \tag{15}$$

where we used that $D_0 \propto D_{\mathrm{rot}}$ as $D_{\mathrm{rot}} \to 0$. The numerical values nicely follow the prediction asymptotically as shown in Fig. 2.

Summary and conclusion.—We have demonstrated that the long-time translational diffusivity of a chiral active Brownian particle in gravitaxis displays a resonance for the external torque approaching the intrinsic angular drift. The resonance originates from an underlying bifurcation of the classical driven pendulum. There are certain similarities with the giant diffusion in tilted washboard potentials [48], yet our approach of decomposition into eigenfunctions is rather complementary and allows calculating the entire time-dependence of low-order moments and is in spirit closer to Ref. [49]. The connection of the resonance to the vanishing low-lying eigenvalues is uncovered and an intuitive picture in terms of a competition between a barrier-dominated and a critical-fluctuation-dominated regime is developed.

The harmonic approximation is surprisingly accurate for the variance as well as for the diffusivity, despite ignoring the rare activation processes over the barrier. We conclude that far above the bifurcation, the orientation performs only small fluctuations most of the time close to the minimum of the effective potential. Then the diffusion coefficient for the translational diffusion remains also small. Yet, approaching the bifurcation these fluctuations become more significant as the confining angular potential becomes softer yielding a significant enhancement of the diffusivity. For too large angular fluctuations the harmonic approximation breaks down as barrier-crossing events become important. After such barrier crossings the orientation quickly completes a full turn until getting stuck again. From the accurateness of the harmonic oscillator description we conclude that these fast events do not significantly contribute to the diffusivity. The essence of the resonance is thus due to the enhancement of small fluctuations as provided by the orientational diffusion coefficient exploring a softening potential as the bifurcation is approached.

Our theoretical work makes detailed predictions for active motion of chiral agents in external fields that can be tested in experiments, both for artificial and biological asymmetric microswimmers. The method is readily extended to calculate higher moments such as

the skewness, the non-Gaussian parameter, or the complete intermediate scattering function. While we explicitly considered gravitaxis, the underlying equations are rather generic and the analysis and methods presented should transfer with suitable adjustments to other forms of *taxis* at the microscale such as durotaxis [56], chemotaxis [27], thermotaxis [57], or topotaxis [58]. Also, the results could be valuable for the transport phenomena of rigid polymer solutions in a flow near a wall [59].

The resonance is of interest not only for single-particle transport in external fields, but also has implications for the collective motion of chiral active particles with alignment interactions [60–63] provided effective mean-field equations can be derived [64–67] which would be similar in structure to the equations of motion studied here.

Last our Letter has theoretical ramifications on the interplay of the critical slowing down of classical transport close to bifurcations and their smearing by random fluctuations. The evolution of the eigenspectrum also for other bifurcations, including the pitchfork or transcritical bifurcations, should be relevant for various branches of science, such as the physics of the Josephson junction [50] or collective (Kuramoto) synchronization [68].

We thank Christina Kurzthaler for constructive criticism on the manuscript. O. C. is supported by the Austrian Science Fund (FWF): M 2450-NBL. T. F. acknowledges funding by FWF: P 35580-N. The computational results presented have been achieved in part using the HPC infrastructure LEO of the University of Innsbruck.

[1] P. Romanczuk, M. Bär, W. Ebeling, B. Lindner, and L. Schimansky-Geier, Active Brownian particles, Eur. Phys. J. Special Topics **202**, 1 (2012).
[2] J. Elgeti, R. G. Winkler, and G. Gompper, Physics of microswimmers—single particle motion and collective behavior: A review, Rep. Prog. Phys. **78**, 056601 (2015).
[3] C. Bechinger, R. Di Leonardo, H. Löwen, C. Reichhardt, G. Volpe, and G. Volpe, Active particles in complex and crowded environments, Rev. Mod. Phys. **88**, 045006 (2016).
[4] A. Zöttl and H. Stark, Emergent behavior in active colloids, J. Phys. Condens. Matter **28**, 253001 (2016).
[5] G. Gompper *et al.*, The 2020 motile active matter roadmap, J. Phys. Condens. Matter **32**, 193001 (2020).
[6] H. C. Berg and D. A. Brown, Chemotaxis in Escherichia coli analysed by three-dimensional tracking, Nature (London) **239**, 500 (1972).
[7] H. C. Berg and L. Turner, Chemotaxis of bacteria in glass capillary arrays. escherichia coli, motility, microchannel plate, and light scattering, Biophys. J. **58**, 919 (1990).
[8] E. Lauga, W. R. DiLuzio, G. M. Whitesides, and H. A. Stone, Swimming in circles: Motion of bacteria near solid boundaries, Biophys. J. **90**, 400 (2006).
[9] S. S. Merchant *et al.*, The Chlamydomonas genome reveals the evolution of key animal and plant functions, Science **318**, 245 (2007).
[10] A. T. Brown, I. D. Vladescu, A. Dawson, T. Vissers, J. Schwarz-Linek, J. S. Lintuvuori, and W. C. K. Poon, Swimming in a crystal, Soft Matter **12**, 131 (2016).
[11] I. Buttinoni, G. Volpe, F. Kümmel, G. Volpe, and C. Bechinger, Active Brownian motion tunable by light, J. Phys. Condens. Matter **24**, 284129 (2012).
[12] A. Bricard, J.-B. Caussin, N. Desreumaux, O. Dauchot, and D. Bartolo, Emergence of macroscopic directed motion in populations of motile colloids, Nature (London) **503**, 95 (2013).
[13] S. van Teeffelen and H. Löwen, Dynamics of a Brownian circle swimmer, Phys. Rev. E **78**, 020101(R) (2008).
[14] F. J. Sevilla and L. A. Gómez Nava, Theory of diffusion of active particles that move at constant speed in two dimensions, Phys. Rev. E **90**, 022130 (2014).
[15] C. Kurzthaler, S. Leitmann, and T. Franosch, Intermediate scattering function of an anisotropic active Brownian particle, Sci. Rep. **6**, 36702 (2016).
[16] J. Toner, H. Löwen, and H. H. Wensink, Following fluctuating signs: Anomalous active super diffusion of swimmers in anisotropic media, Phys. Rev. E **93**, 062610 (2016).
[17] C. Kurzthaler and T. Franosch, Intermediate scattering function of an anisotropic Brownian circle swimmer, Soft Matter **13**, 6396 (2017).
[18] C. Kurzthaler, C. Devailly, J. Arlt, T. Franosch, W. C. K. Poon, V. A. Martinez, and A. T. Brown, Probing the Spatiotemporal Dynamics of Catalytic Janus Particles with Single-Particle Tracking and Differential Dynamic Microscopy, Phys. Rev. Lett. **121**, 078001 (2018).
[19] G. Volpe, I. Buttinoni, D. Vogt, H.-J. Kümmerer, and C. Bechinger, Microswimmers in patterned environments, Soft Matter **7**, 8810 (2011).
[20] O. Chepizhko and F. Peruani, Diffusion, Subdiffusion, and Trapping of Active Particles in Heterogeneous Media, Phys. Rev. Lett. **111**, 160604 (2013).
[21] D. Takagi, J. Palacci, A. B. Braunschweig, M. J. Shelley, and J. Zhang, Hydrodynamic capture of microswimmers into sphere-bound orbits, Soft Matter **10**, 1784 (2014).
[22] M. Zeitz, K. Wolff, and H. Stark, Active Brownian particles moving in a random Lorentz gas, Eur. Phys. J. E **40**, 23 (2017).
[23] C. Reichhardt and C. J. Olson Reichhardt, Active matter transport and jamming on disordered landscapes, Phys. Rev. E **90**, 012701 (2014).
[24] C. Reichhardt and C. J. O. Reichhardt, Negative differential mobility and trapping in active matter systems, J. Phys. Condens. Matter **30**, 015404 (2018).
[25] O. Chepizhko and T. Franosch, Ideal circle microswimmers in crowded media, Soft Matter **15**, 452 (2019).
[26] B. Liebchen and H. Löwen, Synthetic chemotaxis and collective behavior in active matter, Acc. Chem. Res. **51**, 2982 (2018).
[27] H. D. Vuijk, H. Merlitz, M. Lang, A. Sharma, and J.-U. Sommer, Chemotaxis of Cargo-Carrying Self-Propelled Particles, Phys. Rev. Lett. **126**, 208102 (2021).
[28] K. Ērglis, Q. Wen, V. Ose, A. Zeltins, A. Sharipo, P. A. Janmey, and A. Cēbers, Dynamics of magnetotactic bacteria in a rotating magnetic field, Biophys. J. **93**, 1402 (2007).
[29] D. Faivre and D. Schüler, Magnetotactic bacteria and magnetosomes, Chem. Rev. **108**, 4875 (2008).

[30] A. M. Roberts, Mechanisms of gravitaxis in Chlamydomonas, Biol. Bull. **210**, 78 (2006); J. Exp. Biol. **213**, 4158 (2010).

[31] A. J. T. M. Mathijssen, N. Figueroa-Morales, G. Junot, É. Clément, A. Lindner, and A. Zöttl, Oscillatory surface rheotaxis of swimming E. coli bacteria, Nat. Commun. **10** (2019).

[32] B. Liebchen, P. Monderkamp, B. ten Hagen, and H. Löwen, Viscotaxis: Microswimmer Navigation in Viscosity Gradients, Phys. Rev. Lett. **120**, 208002 (2018).

[33] B. ten Hagen, F. Kümmel, R. Wittkowski, D. Takagi, H. Löwen, and C. Bechinger, Gravitaxis of asymmetric self-propelled colloidal particles, Nat. Commun. **5**, 4829 (2014).

[34] Q. Brosseau, F. B. Usabiaga, E. Lushi, Y. Wu, L. Ristroph, M. D. Ward, M. J. Shelley, and J. Zhang, Metallic microswimmers driven up the wall by gravity, Soft Matter **17**, 6597 (2021).

[35] A. I. Campbell, R. Wittkowski, B. ten Hagen, H. Löwen, and S. J. Ebbens, Helical paths, gravitaxis, and separation phenomena for mass-anisotropic self-propelling colloids: Experiment versus theory, J. Chem. Phys. **147**, 084905 (2017).

[36] D. P. Singh, W. E. Uspal, M. N. Popescu, L. G. Wilson, and P. Fischer, Photogravitactic microswimmers, Adv. Funct. Mater. **28**, 1706660 (2018).

[37] F. Rühle and H. Stark, Emergent collective dynamics of bottom-heavy squirmers under gravity, Eur. Phys. J. E **43**, 26 (2020).

[38] F. Fadda, J. J. Molina, and R. Yamamoto, Dynamics of a chiral swimmer sedimenting on a at plate, Phys. Rev. E **101**, 052608 (2020).

[39] J. Palacci, C. Cottin-Bizonne, C. Ybert, and L. Bocquet, Sedimentation and Effective Temperature of Active Colloidal Suspensions, Phys. Rev. Lett. **105**, 088304 (2010).

[40] J. Vachier and M. G. Mazza, Dynamics of sedimenting active Brownian particles, Eur. Phys. J. E **42**, 11 (2019).

[41] F. Ginot, A. Solon, Y. Kafri, C. Ybert, J. Tailleur, and C. Cottin-Bizonne, Sedimentation of self-propelled Janus colloids: Polarization and pressure, New J. Phys. **20**, 115001 (2018).

[42] R. W. Nash, R. Adhikari, J. Tailleur, and M. E. Cates, Run-and-tumble Particles with Hydrodynamics: Sedimentation, Trapping, and Upstream Swimming, Phys. Rev. Lett. **104**, 258101 (2010).

[43] See Supplemental Material at http://link.aps.org/supplemental/10.1103/PhysRevLett.129.228003 for details of the mapping to the noisy driven pendulum, and additional figures of the mean drift and the diffusivity in the presence of additional translational diffusion, which includes Refs. [44, 45].

[44] B. U. Felderhof, Circular Motion of Asymmetric Self-Propelling Particles, Phys. Rev. Lett. **113**, 029801 (2014).

[45] F. Kümmel, B. ten Hagen, R. Wittkowski, D. Takagi, I. Buttinoni, R. Eichhorn, G. Volpe, H. Löwen, and C. Bechinger, Reply:, Phys. Rev. Lett. **113**, 029802 (2014).

[46] B. M. Friedrich and F. Jülicher, The stochastic dance of circling sperm cells: Sperm chemotaxis in the plane, New J. Phys. **10**, 123025 (2008).

[47] H. Löwen, Chirality in microswimmer motion: From circle swimmers to active turbulence, Eur. Phys. J. Special Topics **225**, 2319 (2016).

[48] P. Reimann, C. Van den Broeck, H. Linke, P. Hänggi, J. M. Rubi, and A. Pérez-Madrid, Giant Acceleration of Free Diffusion by Use of Tilted Periodic Potentials, Phys. Rev. Lett. **87**, 010602 (2001); Diffusion in tilted periodic potentials: Enhancement, universality, and scaling, Phys. Rev. E **65**, 031104 (2002).

[49] N. J. López-Alamilla, M. W. Jack, and K. J. Challis, Enhanced diffusion and the eigenvalue band structure of Brownian motion in tilted periodic potentials, Phys. Rev. E **102**, 042405 (2020).

[50] S. H. Strogatz, *Nonlinear Dynamics and Chaos: With Applications to Physics, Biology, Chemistry, and Engineering*, 2nd ed. (CRC Press, Boca Raton, 2018).

[51] H. Risken, *The Fokker-Planck Equation* (Springer, Berlin, Heidelberg, 1989).

[52] This will somewhat change upon reinstating the terms due to translational diffusion that we ignore here.

[53] F. Kümmel, B. ten Hagen, R. Wittkowski, I. Buttinoni, R. Eichhorn, G. Volpe, H. Löwen, and C. Bechinger, Circular Motion of Asymmetric Self-Propelling Particles, Phys. Rev. Lett. **110**, 198302 (2013).

[54] A. Lapolla, D. Hartich, and A. Godec, Spectral theory of fluctuations in time-average statistical mechanics of reversible and driven systems, Phys. Rev. Research **2**, 043084 (2020).

[55] J. Sakurai and J. Napolitano, *Modern Quantum Mechanics* (Addison-Wesley, San Fransico, CA, 2011).

[56] C.-M. Lo, H.-B. Wang, M. Dembo, and Y. li Wang, Cell movement is guided by the rigidity of the substrate, Biophys. J. **79**, 144 (2000).

[57] S. Auschra, A. Bregulla, K. Kroy, and F. Cichos, Thermotaxis of Janus particles, Eur. Phys. J. E **44** (2021).

[58] K. Schakenraad, L. Ravazzano, N. Sarkar, J. A. J. Wondergem, R. M. H. Merks, and L. Giomi, Topotaxis of active Brownian particles, Phys. Rev. E **101**, 032602 (2020).

[59] J. Park, J. M. Bricker, and J. E. Butler, Cross-stream migration in dilute solutions of rigid polymers undergoing rectilinear ow near a wall, Phys. Rev. E **76**, 040801(R) (2007).

[60] B. Liebchen and D. Levis, Collective Behavior of Chiral Active Matter: Pattern Formation and Enhanced flocking, Phys. Rev. Lett. **119**, 058002 (2017).

[61] D. Levis and B. Liebchen, Micro-flock patterns and macro-clusters in chiral active Brownian disks, J. Phys. Condens. Matter **30**, 084001 (2018).

[62] B. Ventejou, H. Chaté, R. Montagne, and X. Q. Shi, Susceptibility of Orientationally Ordered Active Matter to Chirality Disorder, Phys. Rev. Lett. **127**, 238001 (2021).

[63] Q.-L. Lei, M. P. Ciamarra, and R. Ni, Nonequilibrium strongly hyperuniform fluids of circle active particles with large local density fluctuations, Sci. Adv. **5**, eaau7423 (2019).

[64] A. A. Chepizhko and V. L. Kulinskii, On the relation between Vicsek and Kuramoto models of spontaneous synchronization, Physica (Amsterdam) **389A**, 5347 (2010).

[65] F. Peruani, A. Deutsch, and M. Bär, A mean-field theory for self-propelled particles interacting by velocity alignment mechanisms, Eur. Phys. J. Special Topics **157**, 111 (2008).

[66] J. A. Pimentel, M. Aldana, C. Huepe, and H. Larralde, Intrinsic and extrinsic noise effects on phase transitions of network models with applications to swarming systems, Phys. Rev. E **77**, 061138 (2008).

[67] F. Bolley, J. A. Cañizo, and J. A. Carrillo, Mean-field limit for the stochastic vicsek model, Appl. Math. Lett. **25**, 339 (2012).

[68] J. A. Acebrón, L. L. Bonilla, C. J. Pérez Vicente, F. Ritort, and R. Spigler, The Kuramoto model: A simple paradigm for synchronization phenomena, Rev. Mod. Phys. **77**, 137 (2005).